2001

A Glu-496 to Ala polymorphism leads to loss of function of the human P2X7 receptor

Ben J. Gu
Test Research Company

Weiyi Zhang
University of Sydney

Rebecca A. Worthington
University of Sydney

Ronald Sluyter
University of Wollongong, rsluyter@uow.edu.au

L Phuong Dao-Ung

See next page for additional authors

Publication Details

Gu, B. J., Zhang, W., Worthington, R. A., Sluyter, R., Dao-Ung, L., Petrou, S., Barden, J. A. & Wiley, J. (2001). A Glu-496 to Ala polymorphism leads to loss of function of the human P2X7 receptor. Journal of Biological Chemistry, 276 (14), 11135-11142.

A Glu-496 to Ala polymorphism leads to loss of function of the human P2X7 receptor

Abstract

P2X(7) receptor is a ligand-gated cation-selective channel that mediates ATP-induced apoptosis of cells of the immune system. We and others have shown that P2X(7) is nonfunctional both in lymphocytes and monocytes from some subjects. To study a possible genetic basis we sequenced DNA coding for the carboxyl-terminal tail of P2X(7). In 9 of 45 normal subjects a heterozygous nucleotide substitution (1513A-->C) was found, whereas 1 subject carried the homozygous substitution that codes for glutamic acid to alanine at amino acid position 496. Surface expression of P2X(7) on lymphocytes was not affected by this E496A polymorphism, demonstrated both by confocal microscopy and immunofluorescent staining. Monocytes and lymphocytes from the E496A homozygote subject expressed nonfunctional receptor, whereas heterozygotes showed P2X(7) function that was half that of germline P2X(7). Results of transfection experiments showed that the mutant P2X(7) receptor was nonfunctional when expressed at low receptor density but regained function at a high receptor density. This density dependence of mutant P2X(7) function was also seen on differentiation of fresh monocytes to macrophages with interferon-gamma, which up-regulated mutant P2X(7) and partially restored its function. P2X(7)-mediated apoptosis of lymphocytes was impaired in homozygous mutant P2X(7) compared with germline (8.6 versus 35.2%). The data suggest that the glutamic acid at position 496 is required for optimal assembly of the P2X(7) receptor.

Keywords

p2x7, human, function, loss, leads, polymorphism, receptor, ala, glu, 496

Disciplines

Life Sciences | Physical Sciences and Mathematics | Social and Behavioral Sciences

Publication Details

Gu, B. J., Zhang, W., Worthington, R. A., Sluyter, R., Dao-Ung, L., Petrou, S., Barden, J. A. & Wiley, J. (2001). A Glu-496 to Ala polymorphism leads to loss of function of the human P2X7 receptor. Journal of Biological Chemistry, 276 (14), 11135-11142.

Authors

Ben J. Gu, Weiyi Zhang, Rebecca A. Worthington, Ronald Sluyter, L Phuong Dao-Ung, Stephen Petrou, J A. Barden, and James Wiley

JBC Papers in Press. Published on January 9, 2001 as Manuscript M010353200

A GLU (496) TO ALA POLYMORPHISM LEADS TO LOSS OF FUNCTION OF THE HUMAN $P2X_7$ RECEPTOR

Ben J. Gu[1] , Weiyi Zhang[1], Rebecca A. Worthington[2], Ronald Sluyter[1], Phuong Dao-Ung[1], Steven Petrou[3], Julian A. Barden[2] and James S. Wiley[1]

from the Departments of Medicine[1], Anatomy and Histology[2], University of Sydney, NSW and Department of Physiology[3], University of Melbourne, Parkville, VIC, Australia.

Running Title: A polymorphism confers loss of function of $P2X_7$.

Correspondence: Professor J.S. Wiley, Clinical Sciences Building, Nepean Hospital, Penrith, NSW 2750, Australia
Tel: 61-2-473-43277
Fax: 61-2-473-43432
Email: wileyj@medicine.usyd.edu.au

ABSTRACT

The $P2X_7$ receptor is a ligand-gated cation selective channel which mediates ATP-induced apoptosis of cells of the immune system. We and others have shown that $P2X_7$ is non-functional both in lymphocytes and monocytes from some subjects. To study a possible genetic basis we sequenced DNA coding for the carboxyl terminal tail of $P2X_7$. In 9 of 45 normal subjects a heterozygous nucleotide substitution (A1513C) was found while 1 subject carried the homozygous substitution which codes for glutamic acid to alanine at amino acid position 496. Surface expression of $P2X_7$ on lymphocytes was not affected by this Glu496Ala polymorphism demonstrated both by confocal microscopy and immunofluorescent staining. Monocytes and lymphocytes from the Glu496Ala homozygote subject expressed non-functional receptor while heterozygotes showed $P2X_7$ function which was half that of germline $P2X_7$. Results of transfection experiments showed the mutant $P2X_7$ receptor was non-functional when expressed at low receptor density but regained function at a high receptor density. This density-dependence of mutant $P2X_7$ function was also seen on differentiation of fresh monocytes to macrophages with interferon-γ which upregulated mutant $P2X_7$ and partially restored its function. $P2X_7$-mediated apoptosis of lymphocytes was impaired in homozygous mutant $P2X_7$ compared with germline (8.6% versus 35.2%). The data suggest that the glutamic acid at position 496 is required for optimal assembly of the $P2X_7$ receptor.

INTRODUCTION

Purinergic $P2X_7$ receptors are ligand-gated cation channels, present on cells of the immune and haemopoietic system, which have been shown to mediate the ATP-induced apoptotic death of monocytes (1) macrophages (2) and lymphocytes (3,4). The $P2X_7$ receptor family have two transmembrane domains with intracellular amino and carboxyl termini and an oligomeric structure in the plasma membrane based on trimeric or larger complexes of identical subunits (5). Moreover the P2X7 receptor does not appear to form heteropolymers with other P2X subtypes(6). The genes for both the rat and human $P2X_7$ receptors have now been cloned and show extensive homology (30 – 40%) with the other members of the P2X receptor family, although $P2X_7$ differs in having a long carboxyl terminus of 240 amino acids from the inner membrane face (7). The genomic structure of $P2X_7$ consists of 13 exons with exon 12 and exon 13 coding for the carboxyl terminal tail of this molecule. There is strong evidence that this long carboxyl terminus is necessary for the permeability properties of the $P2X_7$ receptor since truncation of this tail abolishes ATP induced uptake of the fluorescent dye YoPro-1 (8). Studies of $P2X_7$ of monocyte-macrophages or of lymphocytes as well as HEK-293 cells expressing the cDNA for $P2X_7$ have shown features which are most unusual for a channel. These include the slow further dilatation following channel opening (9) and the activation of various proteases including membrane metalloproteases (10) and intracellular caspases (2,11). The fully dilated state of the $P2X_7$ pore accepts ethidium cation (314 Da) as a permeant and since ethidium fluorescence is enhanced on binding to nucleic acids the technique of flow cytometry allows a sensitive measurement of the initial rate of permeant uptake which is essentially unidirectional(9). In normal leucocytes a close correlation has been found between ATP induced ethidium uptake and the surface expression of $P2X_7$ receptors measured by the binding of a FITC-conjugated antibody to the extracellular domain of this receptor(12).

There is increasing evidence that a genetic factor plays a role in the functional phenotype of the $P2X_7$ receptor. Thus, Lammas and colleagues (13) have shown that ATP-induced uptake of the dye lucifer yellow into monocytes was minimal in 2 out of 19 normal donors while our group has shown a lack of $P2X_7$ function in both lymphocytes and monocytes in 3 out of 12 patients with B-cell chronic lymphocytic leukaemia (CLL) despite strong

expression of the $P2X_7$ protein (12). These results led us to search for non-functional $P2X_7$ receptors in a large cohort of normal subjects and study its possible genetic basis. The results show a single nucleotide polymorphism is present at low frequency in the Caucasian population and codes for a glutamic acid to alanine substitution at amino acid 496. Homozygosity for the polymorphism produces non-functional $P2X_7$ protein while the heterozygous state gives cells with half the function of cells with germline $P2X_7$ protein.

MATERIALS AND METHODS

Materials

ATP, BzATP (2',3'-O-(4-benzoyl)benzoyl ATP), ethidium bromide, barium chloride, digitonin, D-glucose, BSA (bovine serum albumin), RPMI1640 medium, poly-L-lysine, gentamicin, 7-AAD (7-amino-actinomycin D) and FluoroTag FITC Conjugation Kit were purchased from Sigma Chemical Co (St Louis, MO). Ficoll-Hypaque (density 1.077) and GFX^{TM} PCR DNA and Gel Band Purification Kit was obtained from Amersham Pharmacia (Uppsala, Sweden). FITC (fluorescein isothiocyanate) and RPE (R-phycoerythrin) conjugated negative control antibodies, mouse anti-human CD3, CD14, CD16, CD19 antibodies, and RPE-Cy5 (R-phycoerythrin-Cy5) conjugated mouse anti-human CD19 antibody were from Dako (Carpinteria, CA). Cy2-conjugated donkey anti-mouse IgG antibody was from Jackson ImmunoResearch (West Grove, PA) . Hepes and LipoFectamine^{TM} 2000 reagent, Taq DNA polymerase, Opti-MEM I medium, fetal calf serum (FCS) and normal horse serum were from Life Technologies, Inc. (Galthersburg, MD). Wizard Genomic DNA Purification Kit was bought from Promega (Madison, WI). ABgene Total RNA Isolation Reagent was from Advanced Biotechnologies Ltd (Surrey, U.K.). QIAquick Gel Extraction Kit was from QIAGEN Pty Ltd (Clifton Hill, Vic, Australia). QuikChange^{TM} Site-Directed Mutagenesis Kit was purchased from Stratagene (La Jolla, CA).

Antibody production and preparation. Two types of mouse anti-human $P2X_7$ receptor monoclonal antibodies (mAbs, clone L4 and B2) were used in this study. L4 was prepared from hybridoma supernate by chromatography on Protein A Sepharose Fast Flow as described previously (14). Purified B2 was kindly provided by Dr Gary Buell. FITC labeling kits were used to conjugate these two $P2X_7$ antibodies according to the manufacturers instructions. The conjugated L4 had 1.2 FITC per IgG and B2 had 1.1 FITC per IgG. Both anti-$P2X_7$ antibodies showed no binding to the surface or cytoplasm of HEK293 cells, a cell line which does not express this receptor in sub confluent conditions(15). These two mAbs showed similar surface binding to human hemopoietic cells at a saturating concentration of 60 μg/ml. However, L4 strongly blocks $P2X_7$ receptor function (12,14) while B2 inhibits < 7% of $P2X_7$ receptor function (Buell G, unpublished observation).

Source of human leucocytes. Peripheral blood lymphocytes and monocytes were obtained from 45 normal subjects while the patient with B-chronic lymphocytic leukemia (CLL 4) has been reported in our previous study (12). Mononuclear cells were separated on Ficoll-Hypaque and washed once and resuspended in Hepes-buffered NaCl medium (145 mM NaCl, 5 mM KCl, 10 mM Hepes pH 7.5, 5 mM D-glucose, 1 g/L BSA). In experiments on monocyte-derived macrophages, a mononuclear preparation was incubated for 12 hours in plastic flasks, gently washed to remove non-adherent cells and the adherent monocytes cultured for 7 days in RPMI-1640 medium plus 10% human AB serum and 100 ng/ml interferon-γ. Macrophages were then detached by mechanical scraping for flow cytometric analysis.

Cultured HEK-293 cells. Human embryonic kidney cells (HEK- 293) were cultured in RPMI-1640 complete medium supplemented with 10% heat-inactivated fetal calf serum, 2 mM glutamine, and 0.02mg/ml gentamicin.

Ethidium influx measurement by flow cytometry. Cells ($2x10^6$) prelabeled with appropriate fluorophore-conjugated anti-CD mAbs or anti-$P2X_7$ mAb (clone B2) were washed once and resuspended in 1.0 ml HEPES buffered KCl medium (10mM HEPES, 150 mM KCl, 5 mM D-glucose, 0.1% BSA, pH 7.5) at 37^0C. Cells were analysed at 1000 events per second on a FACSCalibur flow cytometer (Becton Dickinson, San Jose, CA) and were gated by forward and side scatter and by cell type specific antibodies. All samples were stirred and temperature controlled at 37^oC using a Time Zero module (Cytek, Fremont, CA). Ethidium (25μM) was added, followed 40 seconds later by addition of 1.0 mM ATP. The linear mean channel of fluorescence intensity for each gated subpopulation over successive 5 seconds intervals was analysed by WinMDI software (Joseph Trotter, version 2.7) and plotted against time. To correct for any slight variation in the performance of the flow cytometer, fluorescent standard beads (Flow Cytometry Standards Corp, Research Triangle Park, NC) were analyzed each day(9).

Cytosolic Ba^{2+} measurements by fluorometry. Lymphocytes ($1x10^7$/mL) were washed once and loaded with 2 μM Fura-2-acetoxymethyl ester by incubation at 37°C for 30 min in Ca^{2+} free Hepes buffered NaCl medium. Cells were washed once and incubated in

Hepes buffered NaCl with 1 mM Ca^{2+} for another 30 min. Lymphocytes were then washed twice and resuspended in 3 mL Hepes buffered KCl medium at a concentration of $2x10^6$/mL. These samples were stirred at 37°C and stimulated with 1 mM ATP after addition of 1.0 mM $BaCl_2$. Entry of Ba^{2+} into cells loaded with fura-2 produces changes almost identical to those produced by Ca^{2+} in the excitation and emission spectra of Fura-2. Fluorescent signals were recorded on a Johnson Foundation Fluorometer with excitation at 340 nm and emission at 500 nm. Calibration of F_{max} and F_{min} was performed after each run by adding 25 μM digitonin followed by 50 mM EGTA. Control experiments showed that addition of ATP did not release Ca^{2+} from the internal stores of lymphocytes suspended in medium containing EGTA.

DNA extraction and PCR. Genomic DNA was extracted from peripheral blood using the Wizard Genomic DNA Purification System. A primer pair was designed within exon 13 of the $P2X_7$ gene to amplify a 356 bp product from genomic DNA. $P2X_7$ oligonucleotides were synthesized by Life Technologies. The forward primer was 5'-ACTCCTAGATCCAGGGATAGCC-3' and the reverse was 5'-TCACTCTTCGGAAACTCTTTCC-3'. PCR amplification (35 cycles of denaturation at 95°C for 45 sec, annealing at 52°C for 45 sec and extension at 72°C for 1 min) produced a fragment of the expected 356 bp size. PCR products were separated in 2% agarose gel and visualised by ethidium bromide staining.

DNA sequencing for PCR products. Amplified PCR products were purified using QIAquick Gel Extraction Kit protocol. Using AmpliTaq FS dye terminator cycle sequencing kit (Perkin-Elmer Applied Biosystems, USA), fluorescence-based cycle sequencing reaction was performed to sequence the PCR products of $P2X_7$ directly from both ends using specific primers. Sequencing electrophoresis was carried out on the ABI PRISM 377 DNA Sequencer and the ABI PRISM Sequencing Analysis software (version 3.0) was used for the analysis.

Site-Directed Mutagenesis. The full-length clone of $hP2X_7$ (GenBank accession number Y09561) was used in these studies. $hP2X_7$ cDNA was kindly provided by Dr. Gary Buell as a *Not I-Not I* insert in pcDNA3 (Invitrogen). $hP2X_7$ was removed from pcDNA3 using a *Not I-Not I* digest and ligated into pCI (Promega), which is a CMV (cytomegalovirus)

driven mammalian expression vector. Mutant A1513C (E496A) was introduced using overlap PCR (Quick Change™ Site-Directed Mutagenesis Kit, Stratagene) using the expression vector pCI-hP2X$_7$ as a template. The P2X$_7$ point mutation was constructed using a pair of complementary mutagenic primers, consisting of the mutagenic codon flanked by sequences homologous to the wild-type strand of the template. After digestion of the parental DNA with *Dpn I*, intact mutation–containing synthesized DNA was transformed into competent DH5α cells. All mutations were confirmed by sequencing.
The primer sequences were as follows:
A1513C (Glu496Ala) forward: GG.TGC.CTG.GAG.G**C**G.CTG.TGC.TGC.CGG;
A1513C (Glu496Ala) reverse: CCG.GCA.GCA.CAG.C**G**C.CTC.CAG.GCA.CC.
Base changes introducing the mutations are in bold type and underlined.

P2X$_7$ transfection into HEK293 cells. Full length P2X$_7$ cDNA in a plasmid vector pcDNA3 or the mutated P2X$_7$ in pCI as above was transfected into HEK-293 cells by the Lipofectamine 2000 Reagent. Transfection experiments always employed the minimum amount of cDNA which gave surface P2X$_7$ expression. After 40 - 44 hours, cells were collected by mechanical scraping in RPMI-1640 medium containing 10% FCS.

Immunofluorescent staining and confocal microscopy Plastic non-adherent mononuclear cells were incubated on poly-L-lysine-coated (0.1 mg/ml) glass coverslips for 60 min. Fixed cells (4% paraformaldehyde) were blocked with 20% horse serum/0.1% bovine serum albumin before incubating with anti-human P2X$_7$ receptor mAb or isotype control antibody and subsequent labeling with Cy2-conjugated donkey anti-murine IgG antibody. Cells were visualised with a Leica TCS NT UV laser confocal microscope system as previously described (16).

ATP-induced cytotoxicity assay Lymphocytes (1 x 10^7/ml) were incubated with 200 μM BzATP for 15 min at 37^{o}C in Hepes buffered NaCl medium, washed once and incubated in RPMI-1640 medium with 10% FCS for 24 hours. Cells were washed once and stained with FITC-anti-CD3 mAb and 7-AAD (20 μg/ml) for 20 min at room temperature. Viable and non-viable cells were measured by flow cytometry as previously described (17).

RESULTS

$P2X_7$ function in monocytes and lymphocytes

Our previous data has shown that $P2X_7$ receptor function in monocyte or lymphocyte subsets can be measured by the ATP-induced uptake of ethidium at 37^{o}C using time-resolved two-color flow cytometry (12). Mononuclear preparations from 32 normal subjects were pre-incubated with appropriate FITC-labeled monoclonal antibodies and ATP-induced uptake of ethidium into gated monocyte and lymphocyte subpopulations was measured. Ethidium uptake through the $P2X_7$ channel/pore was 5-fold greater for monocytes than for B- T- or NK-lymphocytes of normal origin but for all cell types there was variation in the functional response of the $P2X_7$ receptor (Fig.1) One subject showed complete lack of $P2X_7$ function in both monocytes and lymphocytes shown in Fig. 1 by the filled circles. Variability in ATP-induced dye uptake into monocytes has been observed by others (13).

Identification of a single nucleotide polymorphism in the C-terminal tail of $P2X_7$ gene

Since the long carboxyl-terminal tail of the $P2X_7$ receptor regulates its permeability properties, the sequence of genomic DNA corresponding to this region was analysed. Thus a PCR product was amplified directly from DNA between nucleotide 1425 and 1780 of the coding region of the $P2X_7$ gene and the product was sequenced. In 9 of 45 subjects a heterozygous nucleotide substitution (adenine to cytosine) was found at position 1513 while in 1 out of 45 subjects a homozygous A1513C substitution was observed (Fig. 2). Since the fractional frequency of the mutant allele was 11/90 (0.122) in the Caucasian population it fulfils the criterion for a single nucleotide polymorphism. The deduced amino acid change for this mutation is glutamic acid to alanine at amino acid 496 (Glu496Ala) of the $P2X_7$ protein.

The A1513C mutation is present in skin fibroblasts

Skin fibroblasts were cultured from a punch-biopsy of skin from the homozygous normal subject, DNA was extracted and a product amplified using primers for the C-terminal tail of the $P2X_7$ gene. Sequence analysis of the product showed only cytosine to be present at position 1513 (results not shown).

Surface expression of $P2X_7$ is not affected by the polymorphism

Large amounts of $P2X_7$ protein are found in an intracellular location in monocytes and lymphocytes of all subtypes (12) and we studied whether the A1513C mutation may have reduced the surface expression of this receptor. Confocal microscopy showed strong surface expression of the $P2X_7$ receptor on lymphocytes from subjects who were germline or homozygous for this mutation (Fig.3) while monocytes showed a similar strong surface $P2X_7$ expression (data not shown). Flow cytometric measurement of $P2X_7$ expression using a monoclonal antibody to the extracellular domain of $P2X_7$ (14) showed that the surface expression of this receptor on either B- or T-lymphocytes from heterozygous or homozygous patients was not significantly different from B- or T-lymphocytes which were of germline sequence at position 1513 (Table 1).

Correlation of $P2X_7$ function with the polymorphism

The function of $P2X_7$ receptors expressed on lymphocytes or monocytes was compared with the genotype at position 1513 of the $P2X_7$ gene. Typical ethidium uptake curves for monocytes, B- T- and NK-lymphocytes are shown in Fig. 4 for normal subjects each with germline, heterozygous and homozygous DNA at position 1513. A single patient with B-CLL from our previous study (12) and homozygous A1513C is included in Fig. 4 and Table 1 for comparison. Homozygosity for the mutation led to almost complete loss of function of the receptor while heterozygosity for the mutation gave a function approximately half that of the germline $P2X_7$ sequence (Fig. 4a, b, c, d). Measurement of $P2X_7$ function in a larger group of subjects (n = 20, Table 1) showed that the mean ATP-induced ethidium uptake was reduced in heterozygous subjects to half the uptake found in subjects with germline sequence, and this magnitude of reduction was found for the four cell types studied; monocytes ($p<0.001$) B- ($p<0.002$) T- ($p<0.005$) and NK-lymphocytes ($p<0.03$). ATP-induced uptake of Ba^{2+} was also studied into lymphocytes prepared from the subject with homozygous mutant $P2X_7$. These cells failed to respond to ATP (Fig. 5) indicating that the mutant $P2X_7$ channel was non-functional to small inorganic cations as well as ethidium^{+} as permeants(12).

Function of A1513C mutated P2X$_7$ transfected into HEK293

cDNA for germline P2X$_7$ or P2X$_7$ carrying the A1513C mutation was transfected into HEK293 cells to study whether this mutation abolishes function in transfection experiments. At 40 hours after transfection the surface expression of the P2X$_7$ receptor was quantitated by binding of FITC-conjugated mAb (clone B2) and the ATP-induced uptake of ethidium was studied in the same cell population by two-color flow cytometry. Preliminary experiments suggested that the function of the mutated P2X$_7$ depended on the density at which this receptor was expressed on the cell surface. For this reason a gating strategy was adopted in which cells expressing none, low or high density of P2X$_7$ receptors were analysed as three separate populations (Fig. 6a, b, c). The cohort of cells with negative P2X$_7$ expression showed no ATP-induced ethidium uptake with either germline or mutated cDNA (Fig. 6d). The cohort of cells with low expression of the P2X$_7$ receptor showed strong ATP-induced ethidium uptake in the germline P2X$_7$ but the mutant P2X$_7$ had no function (Fig. 6e). However in the cohort of cells with the highest P2X$_7$ surface expression, substantial ATP-induced ethidium uptake was observed both for the germline and to a lesser extent for the mutant P2X$_7$ (Fig. 6f). These data suggest that the impaired function of the P2X$_7$ receptor in cells carrying the Glu496Ala mutation could be reversed when the density of the mutant receptor was increased on the cell surface.

Homozygous Mutant P2X$_7$ regains partial function in macrophages

Differentiation of monocytes into macrophages greatly increases both the expression and function of the P2X$_7$ receptor (18,19). Peripheral blood monocytes were cultured with interferon-γ for 7 days and the function of P2X$_7$ receptor was measured in the CD14$^+$ macrophage population. Macrophages from subjects with germline P2X$_7$ showed an ATP-induced ethidium uptake about 5-fold greater than their precursor monocytes (Fig. 7a). Thus the area under the ATP-induced ethidium uptake curve increased from 28,920 units on day 0 to 160,000 units in day 6 macrophages. Macrophages from a subject homozygous for A1513C polymorphism developed partial P2X$_7$ function compared to the absent function in the precursor monocytes (Fig. 7b; zero units on day 0 to 30,800 units on day 6). Although the P2X$_7$ expression (mean channels fluorescence intensity) on germline monocyte/macrophages increased from 48 to 284 this increase was less in the homozygous mutant cells (from 51 to 96). Thus the functional defect associated with the Glu496Ala

polymorphism in monocyte/macrophages could be partially reversed when the abundance of native $P2X_7$ was increased on the cell surface.

ATP-induced cytotoxicity is impaired by the homozygous $P2X_7$ polymorphism

$P2X_7$ mediated cytotoxicity was studied in lymphocytes from subjects who were germline or homozygous for the Glu496Ala polymorphism. A mononuclear preparation of peripheral blood was exposed to BzATP for 15 min, washed and incubated a further 24 hr prior to assay by two-color flow cytometry using (a) 7-amino-actinomycin D (7-AAD) as a viability dye and (b) FITC-conjugated CD3 mAb to gate on the predominant T-lymphocyte subpopulation. The fluorescent dot-plots (Fig 8) identify two distinct populations of viable cells (lower region) and non-viable cells (upper region) after 24 hr incubation. The % of non-viable cells was markedly reduced in the homozygote $P2X_7$ mutant compared with germline T-cells (Fig 8a,b). In control lymphocytes not exposed to BzATP, the percentage of non-viable cell was 3.2% for germline and 6.6% for homozygote after 24 hr incubation.

DISCUSSION

The data in this study shows that the function of the human $P2X_7$ receptor is affected by a single nucleotide mutation of adenine to cytosine at position 1513 of cDNA which changes glutamic acid to alanine at amino acid position 496. Homozygosity (C/C) for this polymorphic mutation led to almost complete loss of $P2X_7$ function in leukocytes while heterozygosity (A/C) gave a function which was half that of cells with the germline $P2X_7$ sequence. The negative effect of this mutation on $P2X_7$ function was evident in all leukocytes which express surface $P2X_7$, namely monocytes, B-lymphocytes, T-lymphocytes and NK-cells. Polymorphonuclear leukocytes or platelets which have only weak or no surface expression of $P2X_7$ (12) were not tested. The finding that skin fibroblasts from a homozygous A1513C subject also carry only cytosine at position 1513 indicates the constitutional nature of this mutation which affects tissues other than leukocytes. The fractional frequency of the mutant A1513C allele in the normal subjects was 0.122 so that the mutant allele falls within the definition of a single nucleotide polymorphism defined by a prevalence greater than 0.01 (1%) in the population. Application of the Hardy-Weinberg equilibrium to the A1513C allele frequency found at the DNA level yields an expected value of 0.7 homozygotes which is not significantly different to the observed value of 1 (X^2 = 0.21 with one degree of freedom). Single nucleotide polymorphisms are increasingly recognised as a source of genetic variation and their density may be as high as one per kb of cDNA (20). Most of these polymorphisms have a neutral effect on function, but some contribute to loss of protein function such as found with this A1513C allele. In a recent study of B-CLL our group found 3 of 12 patients demonstrated low or absent function of the $P2X_7$ receptor in the malignant B-lymphocytes as well as in the normal monocytes of peripheral blood (12) . One of these three patients carried the A1513C mutant $P2X_7$ allele in homozygous dosage; while the other two patients were germline at this position (Gu, Zhang and Wiley, unpublished). Clearly A1513C is only one of several genetic changes which can inhibit the function of the $P2X_7$ receptor. It has been previously reported that truncation of the long carboxyl-terminal tail of the rat $P2X_7$ receptor abolishes ATP-induced uptake of large fluorescent dyes such as Yo-Pro^{2+} (8) and truncation of the carboxyl terminal tail of the human $P2X_7$ receptor also abolishes ATP-induced channel/pore formation (Gu and Wiley, unpublished). For this reason we sought a loss-of-function mutation in the carboxyl terminus of $P2X_7$.

Truncation of a receptor often leads to failure of its surface expression such as shown for the 10 amino acid deletion in the chemokine receptor CCR5 gene (21) or the 49 amino acid deletion from the carboxyl terminus of the sulfonylurea receptor which prevents trafficking of this receptor and its associated ATP-sensitive K^+ channel to the surface of the pancreatic β-cell (22). However the Glu496Ala polymorphism in $P2X_7$ allows full expression of the mutant receptor on the cell surface as shown in Fig. 3 and Table 1 for both B- and T-lymphocytes.

The polymorphic A1513C mutation of $P2X_7$ changes glutamic acid to alanine at amino acid 496 (Glu496Ala) and the present data suggests that this glutamic acid residue at position 496 is centrally involved in the interactions which lead to formation of the $P2X_7$ channel/pore. The molecular mechanisms underlying the opening of the cation channel and its transition to a fully dilated pore are not resolved. The simplest model for pore dilation is that it is an intrinsic property of the $P2X_7$ receptor that involves a small scale structural change, perhaps in the selectivity filter of the channel (23). Alternative views suggest that pore dilation involves a large scale structural change such as that induced by the dynamic addition of subunits to the existing oligomeric structure (24) or by an interaction with a protein partner, or the activation of a molecularly distinct pore protein (25) by ligated $P2X_7$ receptor. The inability of some oocyte expression systems to display BzATP activated pore formation (26,27) also provides evidence for regulation of the pore dilation. The finding that the homozygous mutant $P2X_7$ receptor is non-functional for both a small cation, permeant Ba^{2+} as well as the larger ethidium$^+$ emphasizes the importance of this glutamic acid at position 496 both for immediate channel opening as well as its dilatation to a pore. The simplest explanation of the present data is that the glutamic to alanine substitution in the mutant $P2X_7$ weakens the electrostatic interactions governing the assembly of the $P2X_7$ channel complex in the plasma membrane.

Transfection of A1513C mutant $P2X_7$ into HEK293 demonstrated that the loss of channel function in mutant $P2X_7$ could be reversed at high levels of surface expression of the mutant receptor. Two-color flow cytometry (Fig. 6) was used to directly compare ethidium influx through the $P2X_7$ pore in transfected cells gated into three subpopulations, those expressing none, those with low and those expressing high levels of this receptor. This gating strategy employed a FITC-conjugated mAb (clone B2) that binds to an

extracellular epitope of $P2X_7$ but does not inhibit the function of the receptor. Thus ATP-induced ethidium uptake was measured on the red (570 nm) channel into two cell populations defined by high and low (R3 and R2 respectively) fluorescence on the green FITC (525 nm) channel. Germline $P2X_7$ showed function at both high and low receptor numbers at the plasma membrane. In contrast the mutant $P2X_7$ was non-functional at low numbers but regained partial function at higher density of expressed receptors. This important finding was confirmed for the native $P2X_7$ receptor which is upregulated when monocytes from peripheral blood are cultured with interferon-γ to produce macrophages (Fig. 7). The function of germline $P2X_7$ was stimulated about 5-fold in macrophages compared with their precursor monocytes, but the mutant $P2X_7$ only regained partial function in macrophages compared with its zero function in precursor monocytes. Increased receptor abundance may explain the partial restoration of mutant $P2X_7$ channel function since raising the receptor numbers in the membrane of either HEK293 cells (Fig. 6) or human macrophages (Fig. 7) would tend to compensate for weakened self associations and promote receptor assembly by a direct mass action effect. Whatever the mechanism of $P2X_7$ assembly in the membrane, the data in Table 1 shows that much of the person-to-person variation in $P2X_7$ function can be explained by the genetic polymorphism at amino acid position 496 of the $P2X_7$ receptor molecule.

Both gain-of-function as well as loss-of-function mutations can affect genes encoding ion channel proteins(23). Thus an asparagine to lysine polymorphism in the third intracellular loop of the human $\alpha 2_A$-adrenergic receptor enhances coupling to G_i in the presence of agonist(28). Three loss-of-function mutations have been identified in the human $K_{1R}6.2$ gene which encodes the two-transmembrane protein subunit of the pancreatic β-cell ATP sensitive K^+ channel(22). Loss-of-function mutations occur in the nompC gene, a six-transmembrane ion channel in *Drosophila* responsible for mechanosensory signalling(29). However, few if any genetic polymorphisms have been previously described in which one allele encodes a non-functional channel.

Extracellular ATP has an emerging role in the immune system since $P2X_7$ activation leads to apoptotic death of thymocytes (30,31), B-lymphocytes (4), macrophages (2) and dendritic cells (32,33). Thus incubation of mononuclear cells from peripheral blood with ATP gave substantial apoptotic death of T-lymphocytes but cell death was greatly

attenuated in T-lymphocytes from the subject with homozygous Glu496Ala $P2X_7$ protein (Fig. 8). There is good evidence that activation of macrophage $P2X_7$ receptors by ATP can produce killing of intracellular *Mycobacteria tuberculosis* by these cells (13,34). Stimulation of phospholipase D appears to be involved in the killing mechanism (35) and one of the consequences of $P2X_7$ activation is stimulation of the activity of phosphatidyl choline-specific phospholipase D (36-40). Other downstream effects of the $P2X_7$ receptor activation may also occur such as the generation of reactive oxygen intermediates and the stimulation of intracellular caspases which not only kill the organism but also lead to the apoptotic death or cytolysis of the host cell. It is possible that the polymorphism described above may be one of the susceptibility factors predisposing individuals to *Mycobacterial* infections. Thus study of the $P2X_7$ knockout mouse (41) and its resistance to certain infectious requiring competent macrophages for control will be important in defining a role for this receptor. Regardless of the clinical associations of the polymorphism at amino acid 496, this loss-of-function mutation affecting the carboxyl terminal tail of $P2X_7$ may help unravel the molecular events leading to channel/pore formation.

ACKNOWLEDGEMENTS

This work was supported by the Sydney University Cancer Research Fund, the NSW Cancer Council, The Leo & Jenny Foundation and the Cecilia Kilkeary Foundation Ltd. We are grateful to Dr Gary Buell and Dr Iain Chessell for gifts of monoclonal antibodies, Dr Zhan-he Wu for fibroblast culture and Ms Shelley Spicer for typing the manuscript.

REFERENCES

1. Grahames, C. B., Michel, A. D., Chessell, I. P., and Humphrey, P. P. (1999) *Br.J.Pharmacol.* **127**(8)**,** 1915-1921
2. Humphreys, B. D., Rice, J., Kertesy, S. B., and Dubyak, G. R. (2000) *J.Biol.Chem.* **275**(35)**,** 26792-26798
3. Chused, T. M., Apasov, S., and Sitkovsky, M. (1996) *J.Immunol.* **157**(4)**,** 1371-1380
4. Peng, L., Bradley, C. J., and Wiley, J. S. (1998) *Chinese Medical Journal* **78**(7)**,** 508-511
5. Nicke, A., Baumert, H. G., Rettinger, J., Eichele, A., Lambrecht, G., Mutschler, E., and Schmalzing, G. (1998) *EMBO J.* **17**(11)**,** 3016-3028
6. Torres, G. E., Egan, T. M., and Voigt, M. M. (1999) *J.Biol.Chem.* **274**(10)**,** 6653-6659
7. Rassendren, F., Buell, G. N., Virginio, C., Collo, G., North, R. A., and Surprenant, A. (1997) *J.Biol.Chem.* **272**(9)**,** 5482-5486
8. Surprenant, A., Rassendren, F., Kawashima, E., North, R. A., and Buell, G. (1996) *Science* **272**(5262)**,** 735-738
9. Wiley, J. S., Gargett, C. E., Zhang, W., Snook, M. B., and Jamieson, G. P. (1998) *Am.J.Physiol.* **275**(5 Pt 1)**,** C1224-C1231
10. Gu, B., Bendall, L. J., and Wiley, J. S. (1998) *Blood* **92**(3)**,** 946-951
11. Ferrari, D., Los, M., Bauer, M. K., Vandenabeele, P., Wesselborg, S., and Schulze-Osthoff, K. (1999) *FEBS Lett.* **447**(1)**,** 71-75
12. Gu, B. J., Zhang, W. Y., Bendall, L. J., Chessell, I. P., Buell, G. N., and Wiley, J. S. (2000) *Am. J. Physiol. Cell Physiol.* **279**(4)**,** C1189-C1197
13. Lammas, D. A., Stober, C., Harvey, C. J., Kendrick, N., Panchalingam, S., and Kumararatne, D. S. (1997) *Immunity* **7**(3)**,** 433-444
14. Buell, G., Chessell, I. P., Michel, A. D., Collo, G., Salazzo, M., Herren, S., Gretener, D., Grahames, C., Kaur, R., Kosco-Vilbois, M. H., and Humphrey, P. P. (1998) *Blood* **92**(10)**,** 3521-3528
15. Chessell, I. P., Michel, A. D., and Humphrey, P. P. (1998) *Br.J.Pharmacol.* **124**(6)**,** 1314-1320
16. Li, G. H., Lee, E. M., Blair, D., Holding, C., Poronnik, P., Cook, D. I., Barden, J. A., and Bennett, M. R. (2000) *J Biol Chem* **275**(37)**,** 29107-29112
17. Philpott, N. J., Turner, A. J., Scopes, J., Westby, M., Marsh, J. C., Gordon-Smith, E. C., Dalgleish, A. G., and Gibson, F. M. (1996) *Blood* **87**(6)**,** 2244-2251
18. Humphreys, B. D., and Dubyak, G. R. (1998) *J.Leukoc.Biol.* **64**(2)**,** 265-273
19. Hickman, S. E., el Khoury, J., Greenberg, S., Schieren, I., and Silverstein, S. C. (1994) *Blood* **84**(8)**,** 2452-2456
20. Collins, A., Lonjou, C., and Morton, N. E. (1999) *Proc.Natl.Acad.Sci.U.S.A.* **96**(26)**,** 15173-15177
21. Biti, R., Ffrench, R., Young, J., Bennetts, B., Stewart, G., and Liang, T. (1997) *Nat.Med.* **3**(3)**,** 252-253
22. Sharma, N., Crane, A., Gonzalez, G., Bryan, J., and Aguilar-Bryan, L. (2000) *Kidney Int* **57**(3)**,** 803-808
23. Lester, H. A., and Karschin, A. (2000) *Annu Rev Neurosci* **23,** 89-125
24. Tatham, P. E., and Lindau, M. (1990) *J.Gen.Physiol.* **95**(3)**,** 459-476
25. Nuttle, L. C., and Dubyak, G. R. (1994) *J.Biol.Chem.* **269**(19)**,** 13988-13996

26. Klapperstuck, M., Buttner, C., Bohm, T., Schmalzing, G., and Markwardt, F. (2000) *Biochim.Biophys.Acta* **1467**(2)**,** 444-456
27. Petrou, S., Ugur, M., Drummond, R. M., Singer, J. J., and Walsh, J. V., Jr. (1997) *FEBS Lett.* **411**(2-3)**,** 339-345
28. Small, K. M., Forbes, S. L., Bridges, K., and Liggett, S. B. (2000) *J.Biol.Chem.* **in press**
29. Walker, R. G., Willingham, A. T., and Zuker, C. S. (2000) *Science* **287**(5461)**,** 2229-34
30. Zheng, L. M., Zychlinsky, A., Liu, C. C., Ojcius, D. M., and Young, J. D. (1991) *J.Cell Biol.* **112**(2)**,** 279-288
31. Nagy, P. V., Feher, T., Morga, S., and Matko, J. (2000) *Immunol.Lett.* **72**(1)**,** 23-30
32. Nihei, O. K., de Carvalho, A. C., Savino, W., and Alves, L. A. (2000) *Blood* **96**(3)**,** 996-1005
33. Coutinho-Silva, R., Persechini, P. M., Bisaggio, R. D., Perfettini, J. L., Neto, A. C., Kanellopoulos, J. M., Motta-Ly, I., Dautry-Varsat, A., and Ojcius, D. M. (1999) *Am.J.Physiol.* **276**(5 Pt 1)**,** C1139-C1147
34. Sikora, A., Liu, J., Brosnan, C., Buell, G., Chessel, I., and Bloom, B. R. (1999) *J.Immunol.* **163**(2)**,** 558-561
35. Kusner, D. J., and Adams, J. (2000) *J.Immunol.* **164**(1)**,** 379-388
36. Kusner, D. J., and Dubyak, G. R. (1994) *Biochem.J.* **304**(Pt 2)**,** 485-491
37. Humphreys, B. D., and Dubyak, G. R. (1996) *J.Immunol.* **157**(12)**,** 5627-5637
38. el-Moatassim, C., and Dubyak, G. R. (1992) *J.Biol.Chem.* **267**(33)**,** 23664-23673
39. Gargett, C. E., Cornish, E. J., and Wiley, J. S. (1996) *Biochem.J.* **313**(Pt 2)**,** 529-535
40. Fernando, K. C., Gargett, C. E., and Wiley, J. S. (1999) *Arch.Biochem&Biophysics* **362**(2)**,** 197-202
41. Solle, M., Labasi, J., Perregaux, D. G., Stam, E., Petrushova, N., Koller, B. H., Griffiths, R. J., and Gabel, C. A. (2001) *J Biol Chem***, 276**, 125-132

Figure Legend

Fig. 1 Variability of $P2X_7$ receptor function in normal human peripheral blood mononuclear cell subsets. Mononuclear preparations (2×10^6/mL) prelabeled with cell type specific antibodies (CD14 for monocytes, CD19 for B-lymphocytes, CD3 for T lymphocytes and CD16 for NK cells) were suspended in Hepes-buffered KCl medium at 37°C. Ethidium (25μM) was added followed 40 s later by 1.0 mM ATP. Mean channel of cell-associated fluorescence intensity was measured for each gated population at 5 s intervals. $P2X_7$ function is shown as arbitrary units of area under ATP-induced ethidium uptake curve in first 5 min incubation.

Fig. 2 Sequence of genomic DNA at the carboxyl terminal tail of the $P2X_7$ gene showing (a) germline (b) A1513C homozygous mutant and (c) A1513C heterozygote. A 356 bp products was amplified by using a primer pair within exon 13 of $P2X_7$ gene (forward: 5'-ACTCCTAGATCCAGGGATAGCC-3'; reverse: 5'-TCACTCTTCGGAAACTCTTTCC-3'). PCR products were purified and sequenced directly from both ends using the same primers.

Fig. 3 Confocal images of $P2X_7$ receptor expression on the surface of lymphocytes. Lymphocytes from normal subjects, either (a) germline or (b) A1513C homozygote, were labeled with anti-$P2X_7$ receptor mAb (clone L4) and subsequently with Cy2-conjugated anti-mouse IgG antibody. Isotype control antibody was included as negative control and showed no staining. Calibration bar is 2 μm.

Fig. 4 Typical ATP-induced ethidium uptake curve in mononuclear cell subsets from normal subjects with germline, A1513C heterozygous and A1513C homozygous $P2X_7$ as indicated. A single patient with B-chronic lymphocytic leukemia who was A1513C homozygous $P2X_7$ is included for comparison. 2×10^6 cells pre-labeled with appropriate FITC-conjugated surface marker antibody were incubated in 1 ml Hepes buffered KCl at 37°C. Ethidium bromide (25 μM)was added followed 40 s later by 1 mM ATP. Mean channel of cell-associated fluorescence intensity was measured at 5 s intervals for (a) monocytes (gated $CD14^+$), (b) B-lymphocytes (gated $CD19^+$), (c) T-lymphocytes (gated $CD3^+$) and (d) NK cells (gated $CD16^+$) population.

Fig. 5 Ba^{2+} influx on lymphocytes from subjects with germline, A1513C homozygous and heterozygous mutant $P2X_7$. Lymphocytes ($6x10^6$) loaded with 2 μM Fura-2-acetoxymethyl ester were resuspended in 3 mL Hepes buffered KCl medium. 1.0 mM Ba^{2+} was added 40 s before stimulation with 1.0 mM ATP as indicated.

Fig. 6 Surface expression (a,b,c) and function (d,e,f) of HEK293 cells transfected transiently with germline and A1513C site-directed mutant human $P2X_7$ cDNA. 1 μg DNA and 6 μl LipoFectamine 2000 reagent was incubated in 300 μl Opti-MEM I medium for 20 min. The mixture was then added to a 25 cm^2 flask containing 5 x 10^6 HEK293 cells in 3 ml medium. Cells were collected after 40~44 hrs, washed once and incubated with 10 μg/ml FITC-conjugated mouse anti-human $P2X_7$ mAb (clone B2) for 15 min at room temperature. Cells were then washed once and resuspended in 1 ml Hepes buffered KCl medium. Ethidium bromide (25 μM)was added followed 40 s later by 1 mM ATP. Mean channel of cell-associated fluorescence intensity was measured at 5 s intervals for gated sub-populations which expressed $P2X_7$ receptors on their surface at (d) zero (e) low (f) high levels. Data were collected at a constant flow rate of 1,000 total events per second. The gating windows R1, R2, R3 were exactly the same for germline and mutant cells. Control experiment showed negative expression and function of $P2X_7$ on native HEK293 cells. Control experiments excluded an inhibitory effect of B2 monoclonal antibody on $P2X_7$ function. Dotted line is isotype control, solid line shows the histogram for FITC - $P2X_7$ mAb in Figs. a, b, c.

Fig. 7 ATP-induced ethidium uptake on fresh monocytes and monocyte derived macrophages from normal subjects with germline and A1513C homozygous $P2X_7$. Monocytes from mononuclear preparations were allowed to adhere to plastic culture flasks overnight and were cultured for another 6 days in medium plus 100 ng/ml interferon-γ. Cells were collected by gentle mechanical scraping and labeled with FITC-anti-CD14 mAb. Linear mean channel fluorescence intensity was measured in each 5 s interval on the gated $CD14^+$ population after 25 μM ethidium and 1 mM ATP were added.

Fig. 8 BzATP-induced cytotoxicity of T-lymphocytes from subjects with germline and A1513C homozygous $P2X_7$. Lymphocytes ($1x10^7$/ml) were incubated with or without 200 μM BzATP in Hepes buffer NaCl medium at 37^oC for 15 min, washed once and resuspended in RPMI-1640 medium with 10% FCS. After 24 hours incubation cells were labeled with FITC-anti-CD3 mAb and the viability dye 7-AAD. The percentage of live cells is shown in the lower region and non-viable cells in the upper region of each dot plot.

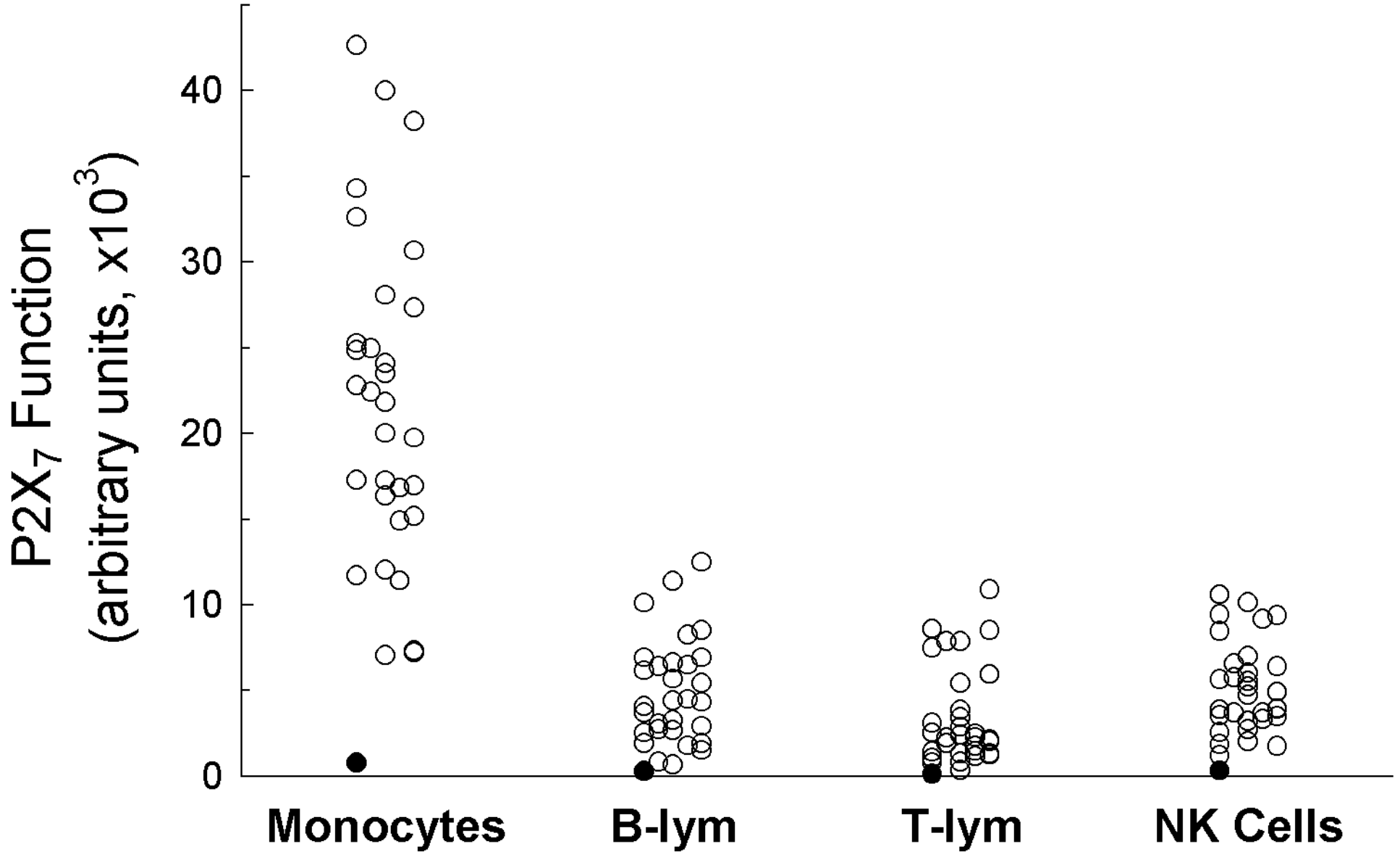
P2X7 Function
(arbitrary units, x10^3)
40
30
20
10
0
Monocytes
B-lym
T-lym
NK Cells

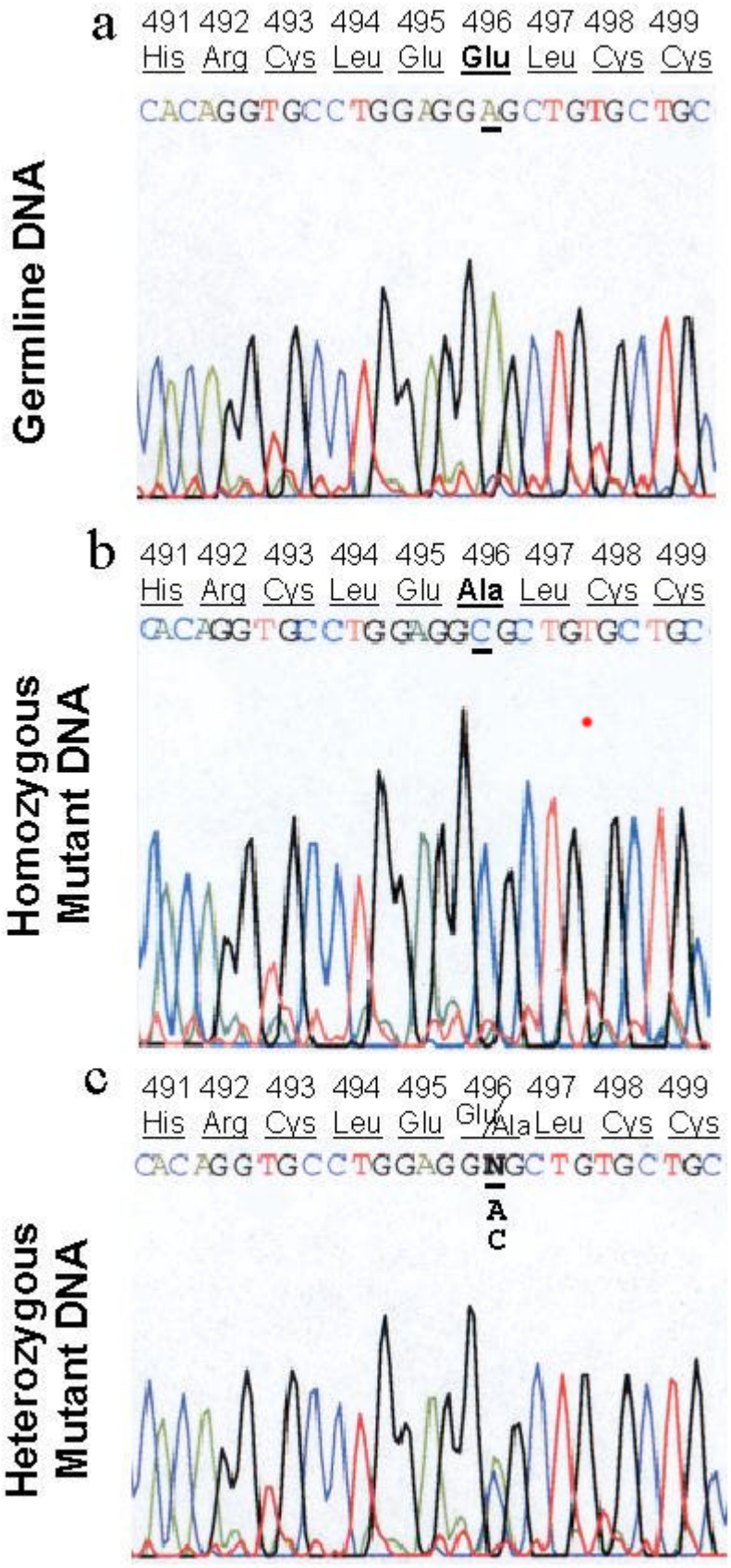
a
491 492 493 494 495 496 497 498 499
His Arg Cys Leu Glu Glu Leu Cys Cys
Germline DNA
b
491 492 493 494 495 496 497 498 499
His Arg Cys Leu Glu Ala Leu Cys Cys
Homozygous Mutant DNA
c
491 492 493 494 495 496 497 498 499
His Arg Cys Leu Glu Glu/Ala Leu Cys Cys
A
C
Heterozygous Mutant DNA

a. Germline

b. A1513C Homozygote

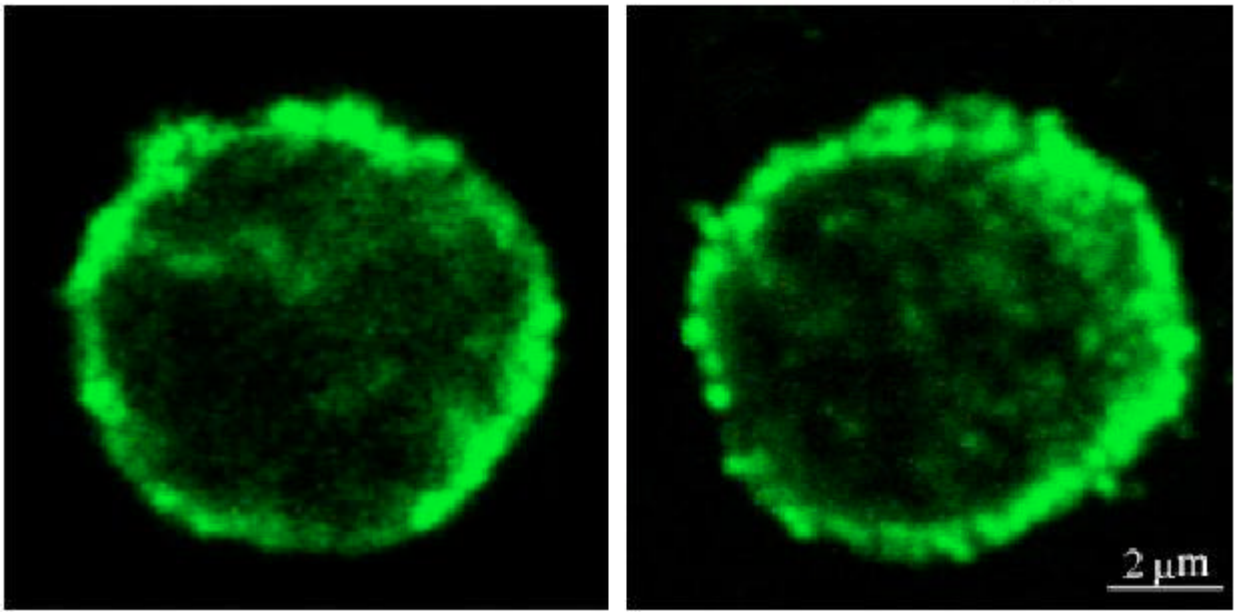

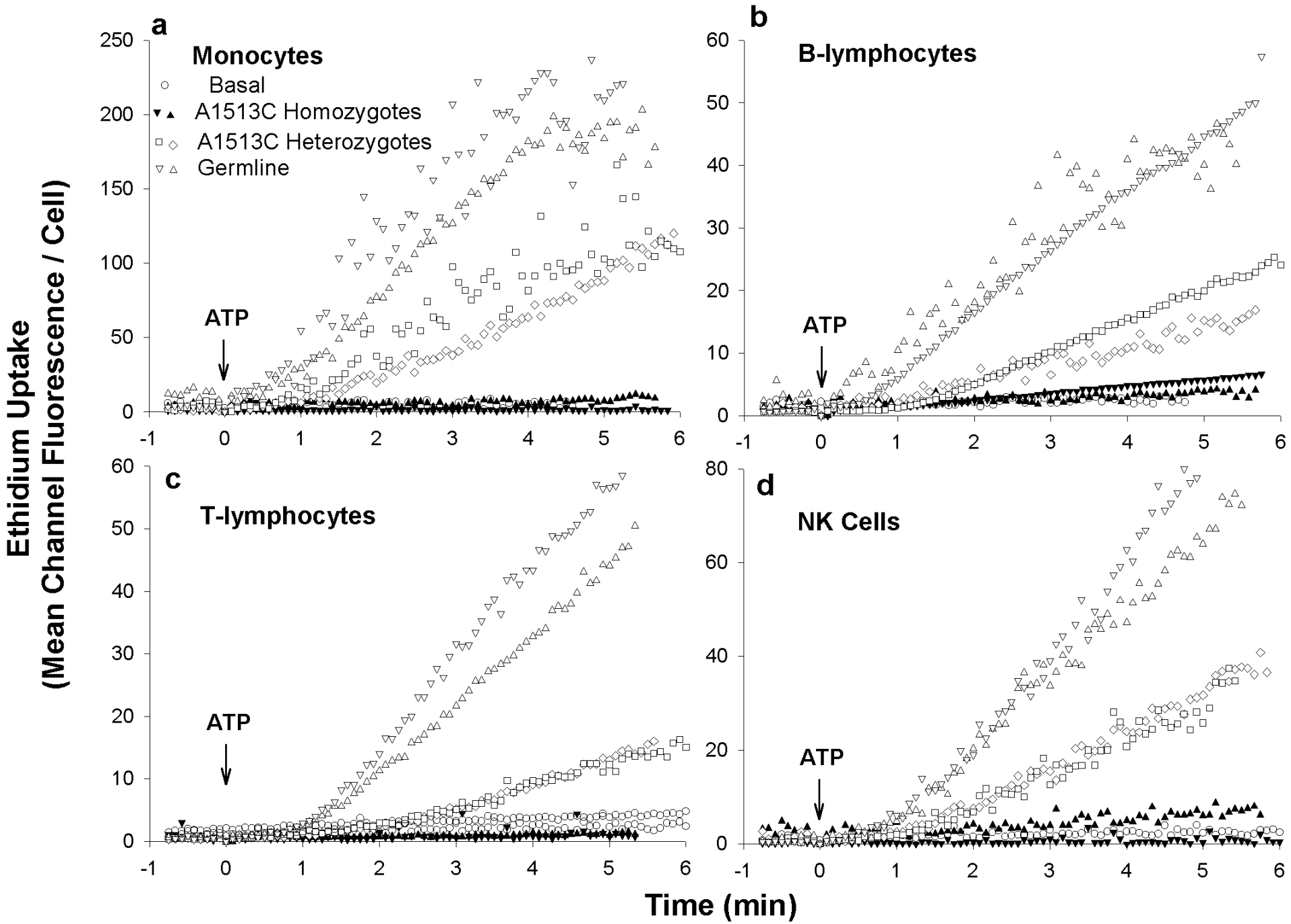
a
Monocytes
Basal
A1513C Homozygotes
A1513C Heterozygotes
Germline
ATP
b
B-lymphocytes
ATP
c
T-lymphocytes
ATP
d
NK Cells
ATP
Ethidium Uptake
(Mean Channel Fluorescence / Cell)
Time (min)

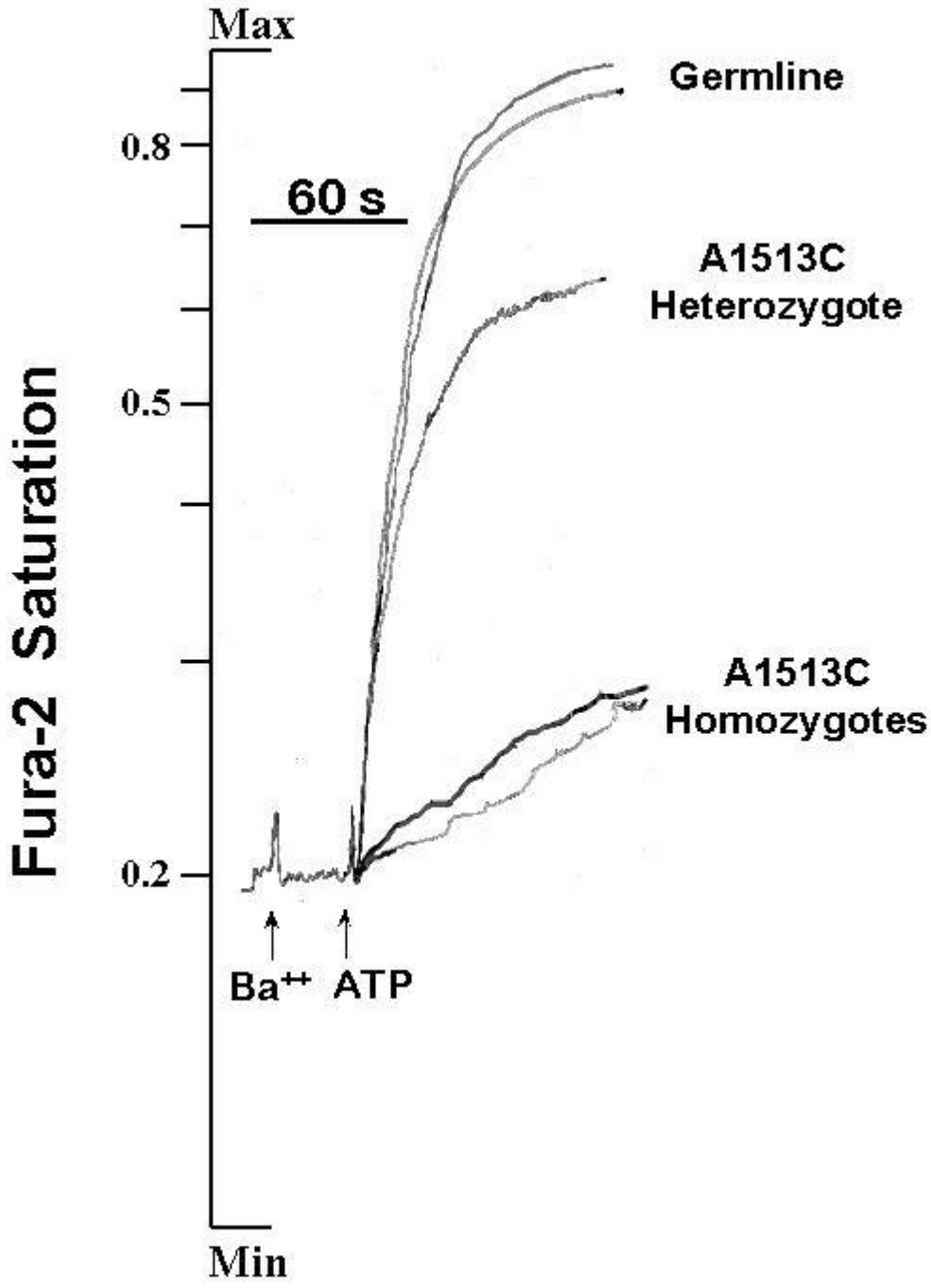
Max
0.8
0.5
0.2
Min
Fura-2 Saturation
60 s
Germline
A1513C
Heterozygote
A1513C
Homozygotes
Ba++
ATP

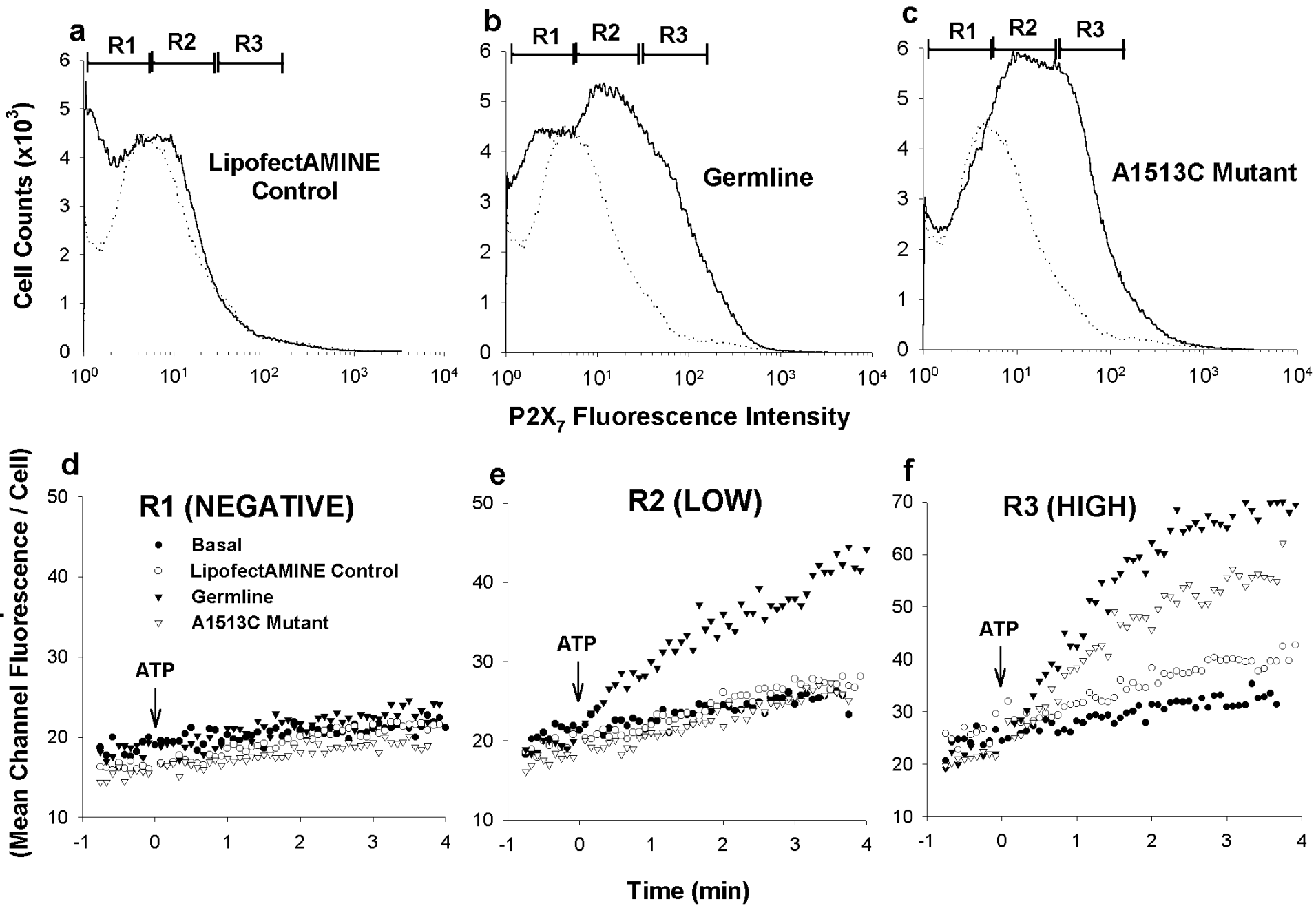
a
R1
R2
R3
LipofectAMINE Control
b
Germline
c
A1513C Mutant
Cell Counts (x10^3)
P2X7 Fluorescence Intensity
d
R1 (NEGATIVE)
Basal
LipofectAMINE Control
Germline
A1513C Mutant
ATP
e
R2 (LOW)
f
R3 (HIGH)
Ethidium Uptake
(Mean Channel Fluorescence / Cell)
Time (min)

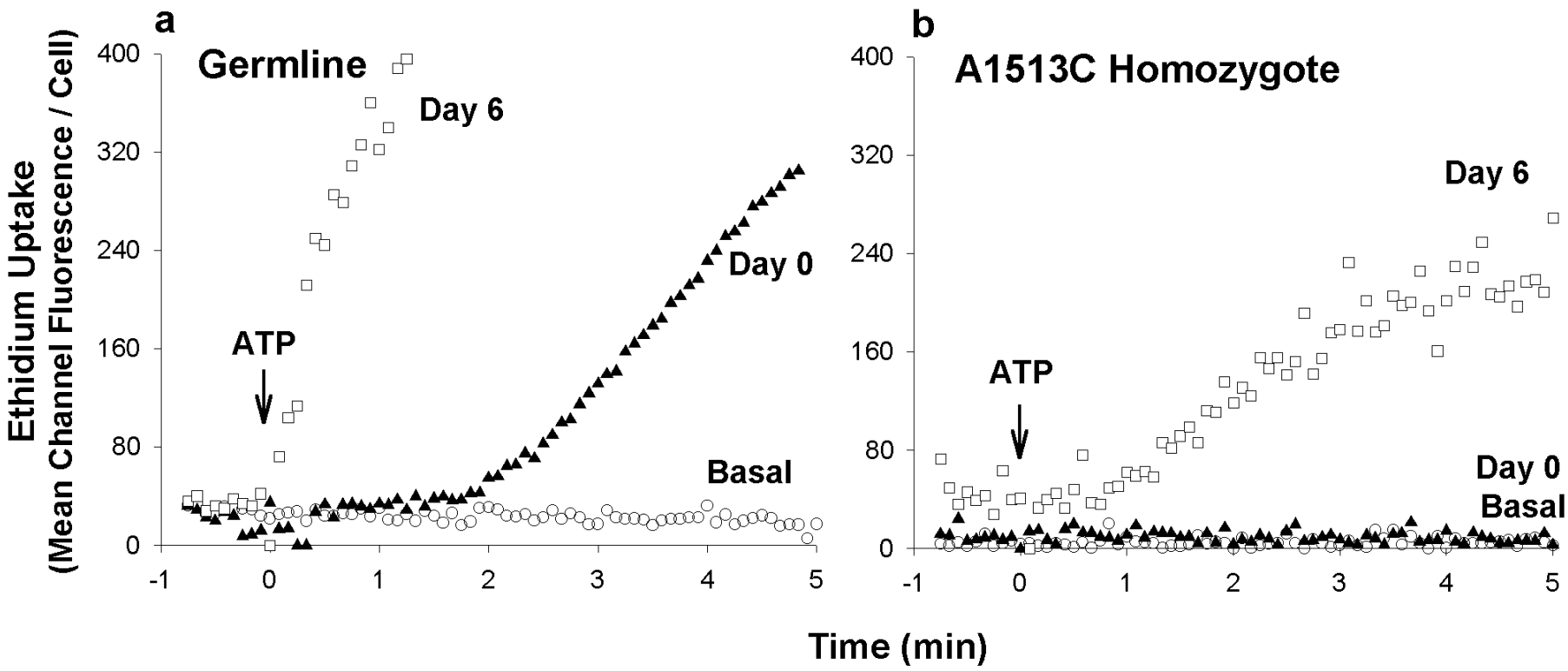
a
Germline
Day 6
Day 0
ATP
Basal
b
A1513C Homozygote
Day 6
ATP
Day 0
Basal
Ethidium Uptake
(Mean Channel Fluorescence / Cell)
400
320
240
160
80
0
-1
0
1
2
3
4
5
Time (min)

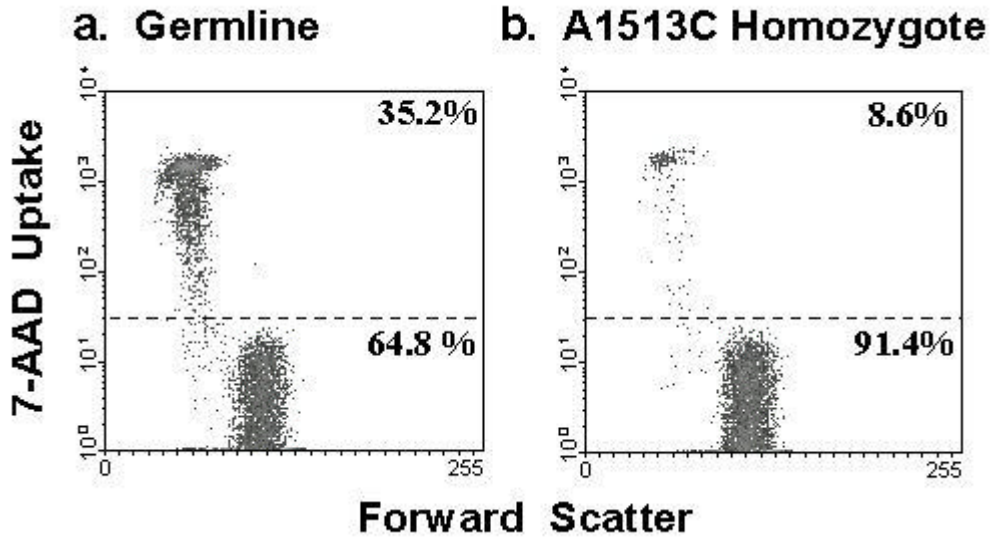
a. Germline
b. A1513C Homozygote
7-AAD Uptake
35.2%
64.8 %
8.6%
91.4%
0
255
Forward Scatter